Hindawi
Advances in Civil Engineering
Volume 2024, Article ID 9942330, 13 pages
https://doi.org/10.1155/2024/9942330

Review Article

Large Section of Soft Rock Gob-Side Entry Retaining Surrounding Rock Control

Xizhi Wang,[1] **Yongjian Zhu**,[1,2,3] **Ping Wang**,[1,2,3] **Heng Ren**,[1] **Peng Li**,[1] **Xianwen He**,[4] **and Jianhua Lv**[4]

[1]*School of Resources and Environment and Safety Engineering, Hunan University of Science and Technology, Xiangtan 411201, China*
[2]*Work Safety Key Lab on Prevention and Control of Gas and Roof Disasters for Southern Coal Mines, Xiangtan 411201, China*
[3]*Hunan Province Key Laboratory of Safe Mining Techniques of Coal Mines, Xiangtan 411201, China*
[4]*Xiaohezui Coal Mine, Sichuan Chuanmei Huarong Energy Co. Ltd., Dazhou 635711, China*

Correspondence should be addressed to Xizhi Wang; 22300101004@mail.hnust.edu.cn

Received 17 August 2023; Revised 18 December 2023; Accepted 4 January 2024; Published 23 January 2024

Academic Editor: Chu Zhaofei

When cutting roof and pressure relief, the impact of blasting is especially obvious on the integrity of the roof of a large-section soft-rock roadway. The reasonable parameters of blasting roof cutting were studied through using Xiaohezui coal mine -12110 roadway as the engineering background. The LS-Dyna simulation results show that: Interval blasting is beneficial to the expansion of interhole cracks and the damage to the perimeter of the hole is smaller than that of adjacent blasting, the lower the charge uncoupling factor, the larger the perimeter of the hole fragmentation zone. The mechanical model of the large-section soft-rock roadway after retrieval was established, the support resistance equation of the roadway side support and the gangue in the extraction area was derived, and the minimum support force required for the roadway side support was solved. According to the site situation, the roadway support scheme for different areas was proposed, and after continuous delamination monitoring of the roof plate, it was found that the amount of roof-plate delamination was finally stabilized within 180 mm after the working face was advanced, and the effect of leaving the roadway was good.

1. Introduction

At present, the mining depth of Chinese mines generally reaches more than 500 m [1–3], and the traditional way of leaving coal pillar to protect the roadway is easy to form stress concentration after the workings are retrieved, which leads to difficulties in maintaining the roadway below the mining area. The technology of gob-side entry retaining has realized coal pillar-free mining, which has many advantages such as improving the coal recovery rate, reducing the amount of roadway excavation, relieving the succession tension, eliminating the stress concentration, and realizing Y-shaped ventilation, and has become the mainstream way of leaving the roadway nowadays. As a means of coal pillarless roadway formation technology, gob-side entry retaining makes full use of the roof rock fragmentation and expansion, not only eliminates the section coal pillar left, but also further utilizes the rock refuse collapsed from the roof of the mining area, so that it can be used as the material of filling body gob-side entry retaining, and can effectively reduce the stress transfer between the roof of the mining area and the roof of the roadway, and improve the stress environment of the roadway.

Most of the technical core of gob-side entry retaining is cutting roof, and the effect of precracking roof cutting often directly affects the adequacy of the rock refuse collapse and pressure relief effect in the mining area and is the key to the success of the gob-side entry retaining, unreasonable parameters of the roof cutting will lead to the suspension of the roof of the mining area after the workface advances without collapse, resulting in the concentration of stress in the solid gang, which is not conducive to the stability of the surrounding rock of the roadway, so the research and development of the roof precracking technology are crucial. A large number of studies have shown [4–9] that for different roof conditions, selecting a suitable depth of roof cutting can not only reduce the stress on the coal gang side and ensure the integrity of the roadway roof, but also reduce the workload of

Table 1: Lithology description of the roof and floor slab of the workface.

No.	Rock name	Thickness (m)	Features
1	Sandy mudstone	8.1	Dark gray medium-thick laminate
2	23-2 Coal	0.15	Dominated by bright coal
3	Sandy mudstone	1.24	Thin gray laminae
4	23 Coal	0.25	Dominated by bright coal
5	Sandy mudstone	1.96	Dark gray medium-thick laminate
6	22 Coal	0.55	Bright coal dominated, fine to medium striped structure
7	Sandy mudstone	1.40	Dark gray medium-thick bedding, interspersed with several layers of coal lines
8	21 Coal	0.87	Bright coal dominated, fine to medium striped structure
9	Muddy siltstone	2.65	Gray medium-thick laminae
10	Fine-grained sandstone	5.53	Gray, undulating laminae, nodular development

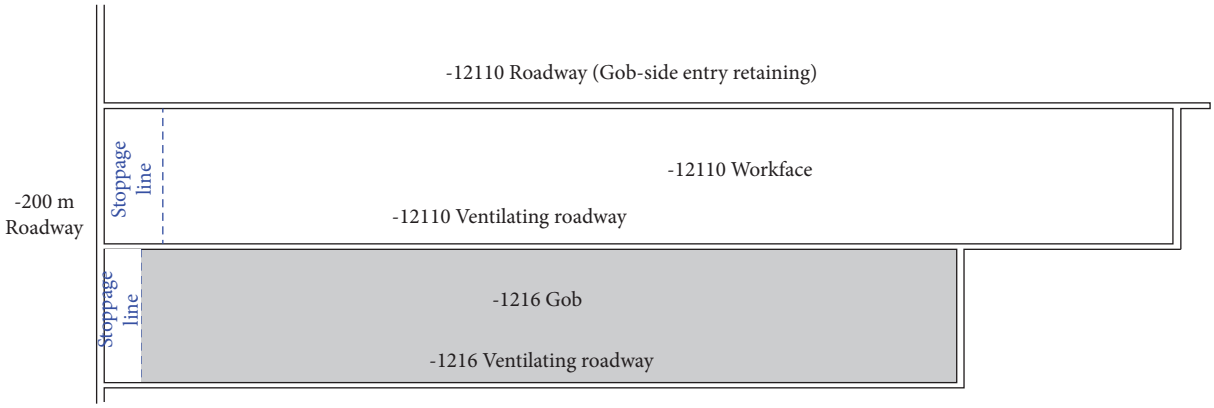

Figure 1: Workface layout.

roof cutting and leaving the roadway to a certain extent. Some scholars have developed a bilateral cumulative tensile explosion technique, He et al. [10] proposed a bilateral cumulative tensile explosion technique to achieve directional precracking of the roadway roof, which effectively controls the displacement of the roof and floor of gob-side entry roadway. Chen et al. [11] established the mechanics model of polyblasting and combined it with the actual site to determine the amount of polyblasting charge and drilling spacing. A number of scholars have used blasting methods as an entry point for their research. Wei et al. [12] explored the influence of pilot holes on crack-expansion patterns during blasting and concluded that pilot holes have a certain control role in the crack expansion. Chen et al. [13] analyzed the action mechanism of pilot holes in the process of blast roof cutting and made an attempt to apply pilot holes to the pressure relief of roof cutting. Tu et al. [14] studied the effect of the superposition effect of blast load between adjacent shell holes on the surrounding rock fracture zone in the process of cutting the roof and unloading the pressure in the engineering background of a thick layer of hard roof, and proposed that the crack evolution between the shell holes was X-shaped.

From a large number of previous research results, it is not difficult to find that changing the state of the roof surrounding rock structure in the roadway and mining area through certain techniques and means can effectively reduce the mine pressure, control the surrounding rock deformation, and reduce the occurrence of mine disasters. The roadway with soft-rock roof, due to the low strength, in the mining causes disturbance more likely bed separation. After cutting the roof of the cross-section of soft-rock roadway to form a load-bearing structure, the deflection is large and the roof accidents are frequent, which increases the frequency of maintenance, increasing the cost of the roadway. Therefore, this paper takes specific engineering practice as the background and initially discusses the optimization scheme of cutting roof and pressure relief parameters for large section soft-rock roadway, to ensure the formation of a load-bearing structure after cutting the roof of a soft-rock roadway, and so as to provide a reference for the promotion and application of gob-side entry retaining technology under complex conditions, especially under the large section and large mining height conditions.

2. Transport Law of Soft-Rock Composite Roof

2.1. Geological Overview. Xiaohezui coal mine -12110 workface is a 21, 22 coal joint mining workface, buried in a depth of about 650 m, the average thickness of 21 coal is 0.87 m, the average thickness of 22 coal is 0.55 m, average dip angle is 3.5°, workface mining height is 3 m, strike length is 1,200 m, and inclination length is 180 m. The rock properties of the roof and floor of the workface are shown in Table 1. The adjacent workface is -1216 workface, -1216 workface has been mined out, as shown in Figure 1. -12110 roadway

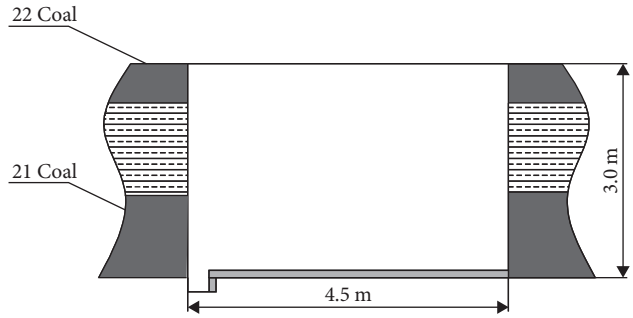

Figure 2: Roadway cross-section.

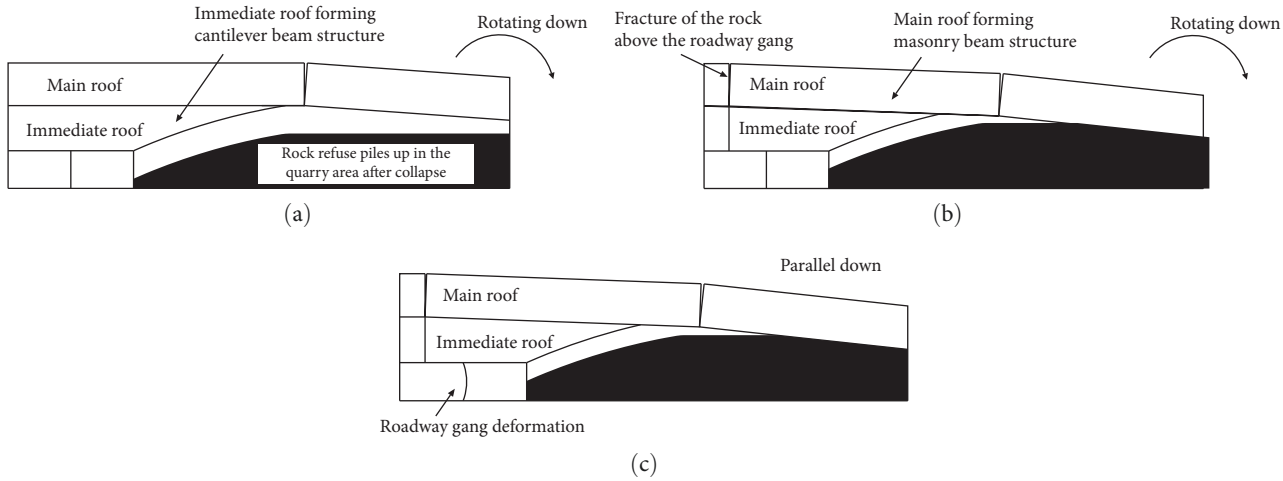

Figure 3: Roof movement process: (a) preliminary activity, (b) transition activities, and (c) anaphase activity.

section is a rectangular, section digging with roadway width, $B = 4.5$ m; roadway height, $H = 3.0$ m; and the proximity area, $S = 13.50$ m^2; in the process of gob-side entry retaining, it is retained as the lower section return airway. Among them, the floor of 21 coal seam is the floor of the roadway, and the roof of 22 coal seam is the roof of the roadway. When the height of the roadway is less than 3.0 m, the floor of 21 coal is broken to reach the height of the roadway, and the roadway section is shown in Figure 2. According to the above geological conditions, the roof of the roadway has the following characteristics:

(1) Due to the existence of 23 coal and 23-2 coal above the roof of the roadway, the immediate roof forms a multilayer coal-soft rock sandwich structure; so, the immediate roof strength is low and it is very easy to delaminate.

(2) The roadway belongs to deeply buried roadway, the surrounding rock is plastic under high stress, and the roadway size is large, which is easy to deform greatly after roadway excavation.

2.2. Soft-Rock Composite Roof Activity Law. The process of soft-rock roadway roof activity is shown in Figure 3. After the workface is retrieved, the stress of the overlying rock layer in the mining area is redistributed to form a mining stress field. The main roof under the influence of mining [15] is divided into initial activity, transitional activity, and later activity by time.

Initial activities of soft-rock roadway are mainly rotational sinking. After the workface was retrieved, with the relocation of the support, the rear rock was overhanged to a large extent. Immediate roof collapse in the mining area under the action of gravity and the support resistance of the alley side support body. The immediate roof above the roadway forms a cantilevered beam structure. The main roof is fractured above the mining area.

Transition activities are still dominated by rotational deformation of the roof. The weight of the main roof overburden is transferred to the solid coal through the immediate roof, forming stress concentration. Under the action of gravity, the main roof further compresses the rock refuse accumulated in the quarry area and continues to sink and deform at a faster rate.

The roof is dominated by parallel sinking in the later activity. The rock refuse collapsed in the extraction area provides a certain support force for the main roof after compaction, and the main roof deformation lasts for a long time, but the sinking speed becomes slower.

From the perspective of the roof transport process, as the immediate roof collapse of the initial activity mining area is not sufficient, collapsed rock refuse accumulation is not

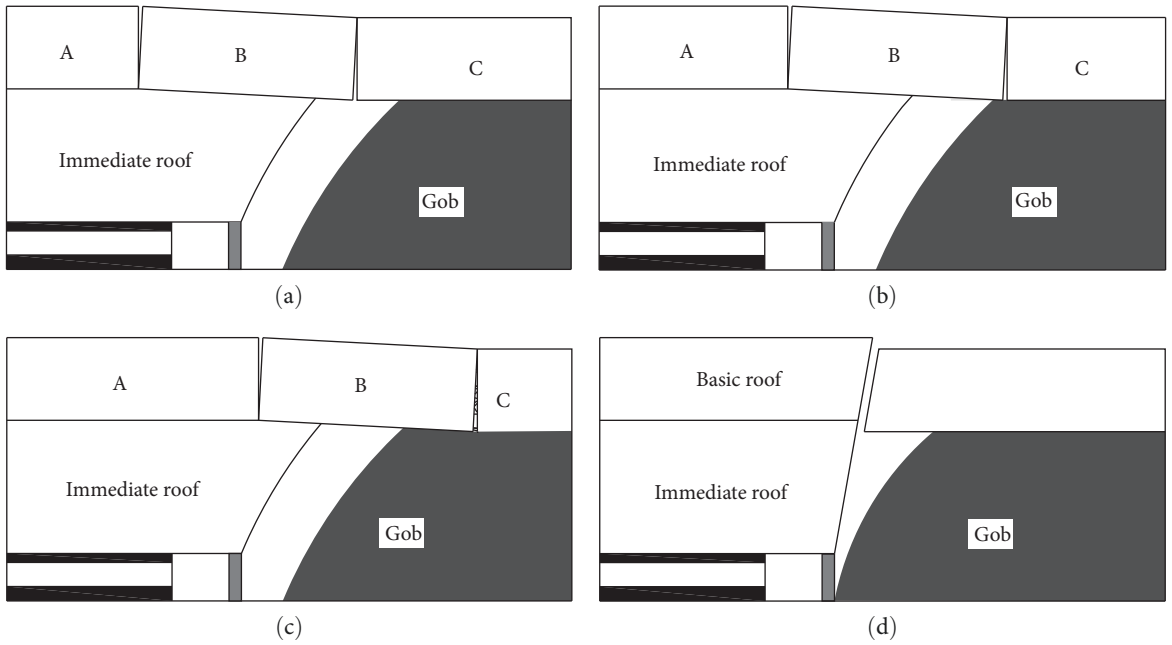

Figure 4: Location of roof rock breakage: (a) breakage above the solid coal side, (b) breakage above the roof of the roadway, (c) breaking above the mining area, and (d) breaking above the mining area after precracking and blasting.

dense, and the roof of the roadway is easy to form a cantilever beam structure. The main roof forms an articulated structure consisting of rock A, rock B, and rock C. The immediate roof of the mining area started to collapse after the working face was advanced. The rock B will sink toward the side of the extraction area, and the support next to the road is further compressed until the rock B touches the rock refuse, and continues to compact the rock refuse in the extraction area. The compacted gangue forms a certain support capacity for rock B, and together with the alley side support and solid coal gang, it forms an effective support for the roof of the roadway, which is further divided into three cases according to the different locations of the roof break, as shown in Figure 4(a)–4(c). The stability of the structure depends mainly on the degree of compaction of the extraction zone and the fracture parameters of the roof rock. The structure was then optimized by using a cutting roof to ensure the stability of the roadway, as shown in Figure 4(d).

3. Mechanical Analysis of the Roof of Soft-Rock Roadway with Large

The key to the technology of cutting the roof and pressure relief without coal column gob-side entry retaining [16] is to cutoff the connection between the roof of the mining area and the roof of the roadway, so that the roof of the roadway forms a short-arm beam structure. On the one hand, it is conducive to the full collapse of the roof of the mining area, which plays the role of filling and sealing the mining area to a certain extent. On the other hand, it is conducive to reducing the support resistance of the alley side, changing the force state of the solid coal gang, and controlling the large deformation of the surrounding rock. Therefore, it is important to determine the initiation and stopping of rock cracking during blasting before modeling the roadway mechanics.

3.1. Calculation of Blasting Parameters. According to fracture mechanics [17], when the stress intensity factor (K_{I}) at the fracture end is greater than the fracture toughness (K_{IC}) of the rock, the rock starts to crack. On the contrary, the rock stops cracking. The stress intensity factor at the crack tip when the crack expands is as follows:

$$K_I = P_0 F \sqrt{\pi (r_b + l_0)} + \sigma_\theta \sqrt{\pi l_0}, \tag{1}$$

where K_{I} is the crack tip stress intensity factor; P_0 is the burst gas pressure; r_{b} is the radius o*f* the gun hole; l_0 is the initial pilot crack length; σ_θ is the annular stress; F is the stress intensity factor correction factor, and

$$F = f\left(\frac{r_b + l_0}{r_b}\right). \tag{2}$$

Therefore, the longer the initial crack length, the larger the stress intensity factor correction factor. F changed a lot when $\frac{r_b+l_0}{r_b} > 1.5$. When $\frac{r_b+l_0}{r_b} < 1.5$, F tended to 1.

When the rock starts to crack, the pressure of the explosive gas along the direction of energy gathering satisfies

$$p_0 > \frac{K_{IC} - \sigma_\theta \sqrt{\pi l_0}}{F \sqrt{\pi (r_b + l_0)}}, \tag{3}$$

while in the direction of nonagglomeration, there are

$$p_0 > \frac{K_{IC}}{F \sqrt{\pi (r_b + l_0)}}. \tag{4}$$

As shown in Figure 5, the bilateral cumulative tensile explosion can guide the crack to crack and expand in a

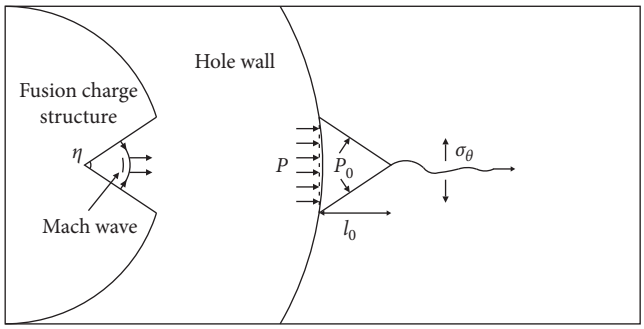

Figure 5: Principle of bilateral cumulative tensile explosion.

Figure 6: Deformation of the roof of the roadway.

certain direction. And the greater the initial jet strength, the longer the initial guided crack produced by rock breaking, the more easily the crack will expand in the intended direction.

In the initial roof cutting and pressure relief in -12110 roadway, the engineering analogy method was used on site to determine the roof-cutting angle of 15°, the depth of roof cutting of 12 m, the hole spacing of 0.4 m, and the hole diameter of 48 mm. Due to technical conditions and cost constraints, the field engineer used Φ32-mm PVC pipe loaded with explosives, the diameter of the emulsion explosive used is Φ32 mm × 330 mm/roll, the mass of individual roll is 300 g, and the loading quantity of each blasting hole is 4.5 kg. Due to the above characteristics of the roadway roof, the roof showed obvious cracks after blasting and cutting of the roof, and the roof in the mining area could collapse sufficiently in time after retrieval, but the roof plate of the roadway sank seriously. The surrounding rock was found to be broken within 5 m above the roof plate after using drilling peep observation, as shown in Figures 6–8. The main reason is that the large span of the roadway and the large blasting charge lead to the expansion of the cracks of undirected blasting to the roof of the roadway, which leads to the sharp sinking of the roof of the large section of the roadway under the influence of blasting and mining.

From the effect of roof cutting on site, the crack disorderly expansion caused by excessive blasting charge and undirected blasting will destroy the integrity of the roof of the roadway leading to difficulty controlling the roof deformation and affecting the original support structure. The bidirectional-shaped charge blasting can be released in the direction set in the blast

Figure 7: Cracking of the roof surface after blast roof cutting.

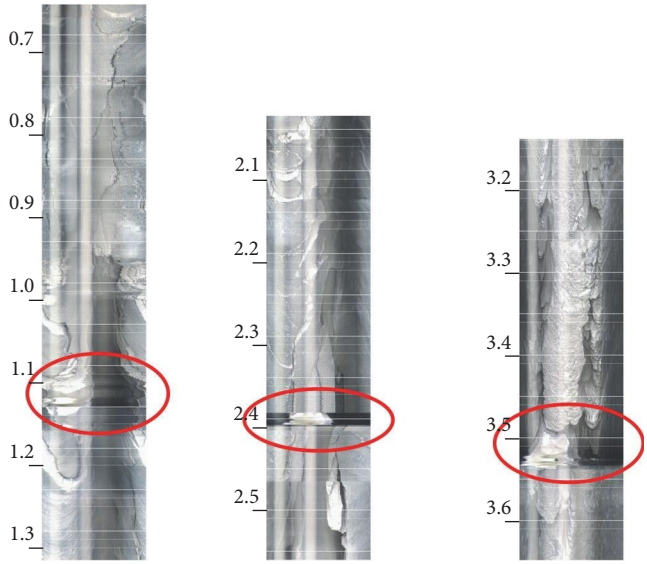

Figure 8: Horizontal misalignment of blast holes.

hole after the explosives are detonated, so that the tensile force in the fissure is greater than the tensile strength of the roof rock thus forming a tangent line to cut the roof while ensuring the integrity of the roof in the tunnel. Therefore, blasting parameters determine whether the roof can be precracked successfully, and reasonable blasting parameters are very important in order to achieve the ideal blasting effect with the economy.

The formula for calculating the charge of blasting holes is as follows [18]:

$$q_e = \frac{\pi}{4} d_c^2 \rho_0 l_e l, \tag{5}$$

where d_c is the charge diameter, m; ρ_0 is the charge density of the shell hole, kg/m^3; l is the length of the shell hole, m; and l_e is the charge factor of the shell hole, and

$$l_e = \left[\frac{8K_{IC}}{\rho_0 D_V \sqrt{\pi a f\left(\frac{a}{r}\right)}}\right]^{\frac{1}{3}} \left(\frac{d_b}{d_c}\right)^2, \tag{6}$$

where K_{IC} is the fracture toughness of the rock, MPa · m$^{\frac{1}{2}}$; D_V is the explosive blast rate, m/s; a is the length of

Table 2: Explosive's parameters.

Density (kg/m^3)	Explosion speed (m/s)	E_0 (GPa)	A (GPa)	B (GPa)	R_1	R_2	ω
1,200	3,600	4.192	214.4	0.182	4.2	0.9	0.15

Table 3: Rock parameters.

Density (kg/m^3)	Bulk modulus (GPa)	Shear modulus (GPa)	Friction (degree)	Tension (MPa)	Cohesion (MPa)
1,200	6.27	2.10	38	0.292	4.2

the guide crack, m; r is the radius of the hole, m; and $f(\frac{a}{r})$ is the shape of the influence factor, can be found in the table. The parameters of the -12110 roadway cutting-roof pressure release are substituted into the above equation and solved for $q_e = 2.1$ kg.

The formula for calculating the gun hole spacing [19] is as follows:

$$E = Kr_b f^{\frac{1}{3}}, \tag{7}$$

where K is the adjustment factor, generally take 10–15, the higher the rock hardness to take the value of the smaller; r_b is the radius of the gun hole; and f is the rock Pratt's coefficient. The actual data measured in the field are substituted to obtain $E = 14 \times 0.025 \times 3^{\frac{1}{3}} \approx 0.5$ m.

The blast hole angle was determined to be 10°, according to the literature [18].

Based on the key layer theory [20], the depth of the roadway cutting roof can be solved as 12 m.

After determining cutting roof parameters using LS-DYNA simulation blasting cutting roof. The algorithm used ALE, the model was analyzed by fluid-structure coupling method, explosives using JWL equation to describe the pressure–volume relationship of the blast products, that is

$$p = A\left(1 - \frac{\omega}{R_1 V}\right)e^{-R_1 V} + B\left(1 - \frac{\omega}{R_2 V}\right)e^{-R_2 V} + \frac{\omega E_0}{V}, \tag{8}$$

where p is the unit pressure of the blast product; V is the relative volume of the blast product; E_0 is the initial internal energy density of the blast product; and A, B, R_1, R_2, and ω are the material constants.

The material of the explosive is MAT_HIGH_EXPLOSIVE_BURN, and the parameters of the explosive are shown in Table 2.

The rock material model uses the RHT model. The model considers the effect of the damage strength of rock material under dynamic load on the impact pressure, strain rate, strain hardening, and damage softening, and uses the equation of state to describe the damage process of rock material under different force states [21]:

Table 4: Air material parameter.

Density (kg/m$^{3)}$	C_0	C_1	C_2	C_3	C_4	C_5	C_6
1,290	0	0	0	0	0.4	0.4	0

Table 5: LS-Dyna simulation blasting scheme.

Number	L (mm)	D (mm)	d (mm)	Blasting method
1	500	48	32	Adjacent blasting
2	500	48	36	Adjacent blasting
3	500	48	40	Adjacent blasting
4	500	48	44	Adjacent blasting
5	500	48	48	Adjacent blasting
6	500	48	32	Interval blasting
7	500	48	36	Interval blasting
8	500	48	40	Interval blasting
9	500	48	44	Interval blasting
10	500	48	48	Interval blasting

$$p = \begin{cases} A_1\theta + A_2\theta^2 + A_3\theta^3 + (B_0 + B_1\theta)\rho_0 e, \theta > 0 \\ T_1\theta + T_2\theta^2 + B_0\rho_0 e, \theta < 0 \end{cases}, \tag{9}$$

where p is the pressure of the material after compression; θ is the volume strain, $\theta = \frac{\rho}{\rho_0} - 1$; ρ is the density of the material during compression; ρ_0 is the initial density of the material; e is the initial internal energy of the material; A_1, A_2, and A_3 are Hugoniot polynomial coefficients; and B_0, B_1, T_1, and T_2 are the parameters of the equation of state. The parameters of the rock are shown in Table 3.

The air material is the MAT_NULL model and EOS_LINEAR_POLYNOMIAL is used to describe the thermodynamic properties of the material:

$$P = (C_0 + C_1\mu + C_2\mu^2 + C_3\mu^3) + (C_4 + C_5\mu + C_6\mu^2)E_0, \tag{10}$$

where μ is the specific volume and C_0–C_6 is the air material parameter, as shown in Table 4.

As shown in Table 5, simultaneous detonation is used to cutting roof, and the length of each blast is 1 m. Two types of adjacent blasting and interval blasting (there are pilot holes between the two holes) are designed, where L is the distance between the holes, D is the diameter of the holes, and d is the

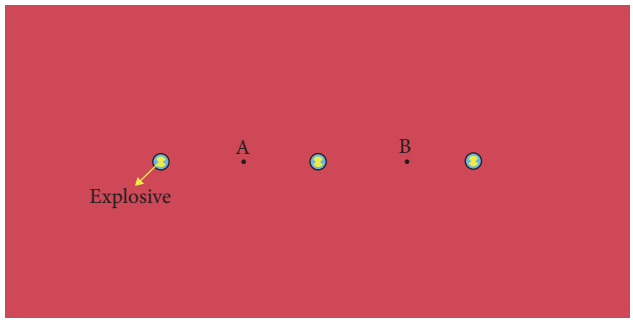

Figure 9: Adjacent blasting.

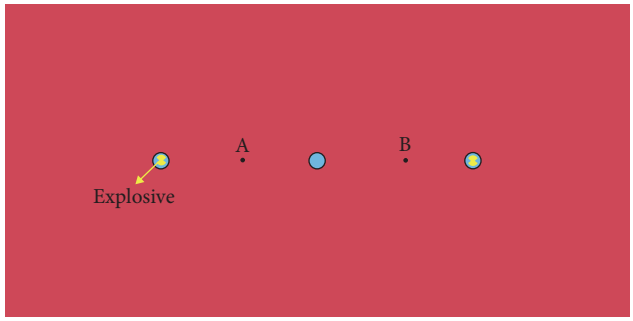

Figure 10: Interval blasting.

diameter of the charge (the ratio of D to d is the uncoupling coefficient of the charge), and the blast holes and monitoring points are arranged as shown in Figures 9 and 10.

Figure 11 shows the change curve of y-directional stress at the monitoring points of different schemes. At 50 μs after the detonation of the explosive, the y-directional stress at the measuring points of 32, 36, and 40 mm diameter of the adjacent blasting hole charge increased to 0.4 GPa; the y-directional stress is increased to 0.45 GPa at the measurement point with a charge diameter of 44 mm; the y-directional stress was increased to 0.63 GPa at the measurement point with a charge diameter of 48 mm. At 50 μs after the detonation of the explosive, the y-directional stress at the measurement points of the interval blasting method increased to 0.14 GPa, and the duration of stress fluctuations in the y-direction was more than 650 μs. The duration of stress fluctuation time in the y-direction is basically the same for different blasting methods when the charge diameter is 32 mm, while the duration of stress fluctuation time in the y-direction is greatly influenced by different blasting methods when the charge diameter is larger than 32 mm. As shown in Figure 11(b)–11(e), the duration of the stress wave in the y-direction can be as long as 1,000 μs and as short as 700 μs when using the interval blasting method, and the duration of the impact of interval blasting is longer than that of adjacent blasting. The y-directional stresses generated during adjacent blasting in 100 μs are much greater than those generated during interval blasting. Therefore, interval blasting has less effect on the perimeter fracture zone of the hole, but has a certain promotion effect on the crack opening.

The crack extensions after blasting under different conditions were obtained during the LS-Dyna calculations for pairs, as shown in Figure 12. During adjacent blasting, blasts with charge diameters of 32 mm and above can form cracks between the holes, and as the charge uncoupling factor decreases, the higher the degree of damage to the cracks formed between the holes. When interval blasting, the hollow hole is used as the guide hole, and the charge diameter is less than 40 mm, the damaged area between the shell holes cannot be penetrated, and no effective crack can be formed between the rocks. The charge diameter greater than or equal to 40 mm can form an effective precrack along the round center line of the shell hole, and the guide hole plays a certain role in guiding the formation and final distribution of cracks. As the charge uncoupling coefficient decreases, the crushing zone of the rock around the hole also gradually expands; so, it is not advisable to choose too low a charge diameter.

3.2. Mechanical Model of the Roadway. After the roadway cut the roof, the immediate roof forms a short-arm beam structure, and the roadway side support plays a bearing role while also cutting off the main roof. The fallen gangue, roadway side support, and roadway gang collaborate to carry the load and form the masonry beam structure.

Before building a mechanical model of the roadway, the following assumptions are made about the roadway:

First, the basic roof has been cutoff, the roof is in late activity, and only parallel subsidence exists;

Second, the gangue that collapses from the roof after recovery fills the quarry area and provides some support to the rock above it;

Third, neglecting the horizontal forces between the roof and the roadside support and between the roof and the overlying rock layer;

Fourth, the overlying rock gravity is considered as a uniform load applied on the roof of the roadway;

Fifth, ignoring the impact of the roadway support structure on the roof.

In Figure 13, P is the load exerted by the overlying rock layer, P_0 is the support resistance of the coal gang to the roof, p_1 is the support resistance of the support next to the roadway after cutting the roof, p_2 is the support force of the collapsed gangue to the immediate roof, p_3 is the support force of the collapsed gangue to the basic roof, w is the width of the roadway, and l is the width of the support next to the roadway, and the width of the loose zone of the lane gang is

$$x = \frac{\lambda m}{2\tan\varphi} \ln\left(\frac{k\gamma H + \frac{c}{\tan\varphi}}{\frac{c}{\tan\varphi} + \frac{P_x}{\lambda}}\right), \tag{11}$$

where c and φ are the cohesion and friction, respectively; m is the thickness of coal seam; λ is the lateral pressure coefficient; k is the maximum concentrated stress coefficient; γ is the capacity weight of surrounding rock; H is the burial depth; and P_x is the compressive strength of coal gang.

When the roof activity is in anaphase activity, the static equilibrium method is used to analyze the force on the tunnel surrounding rock and establish the mechanical equilibrium equation as follows:

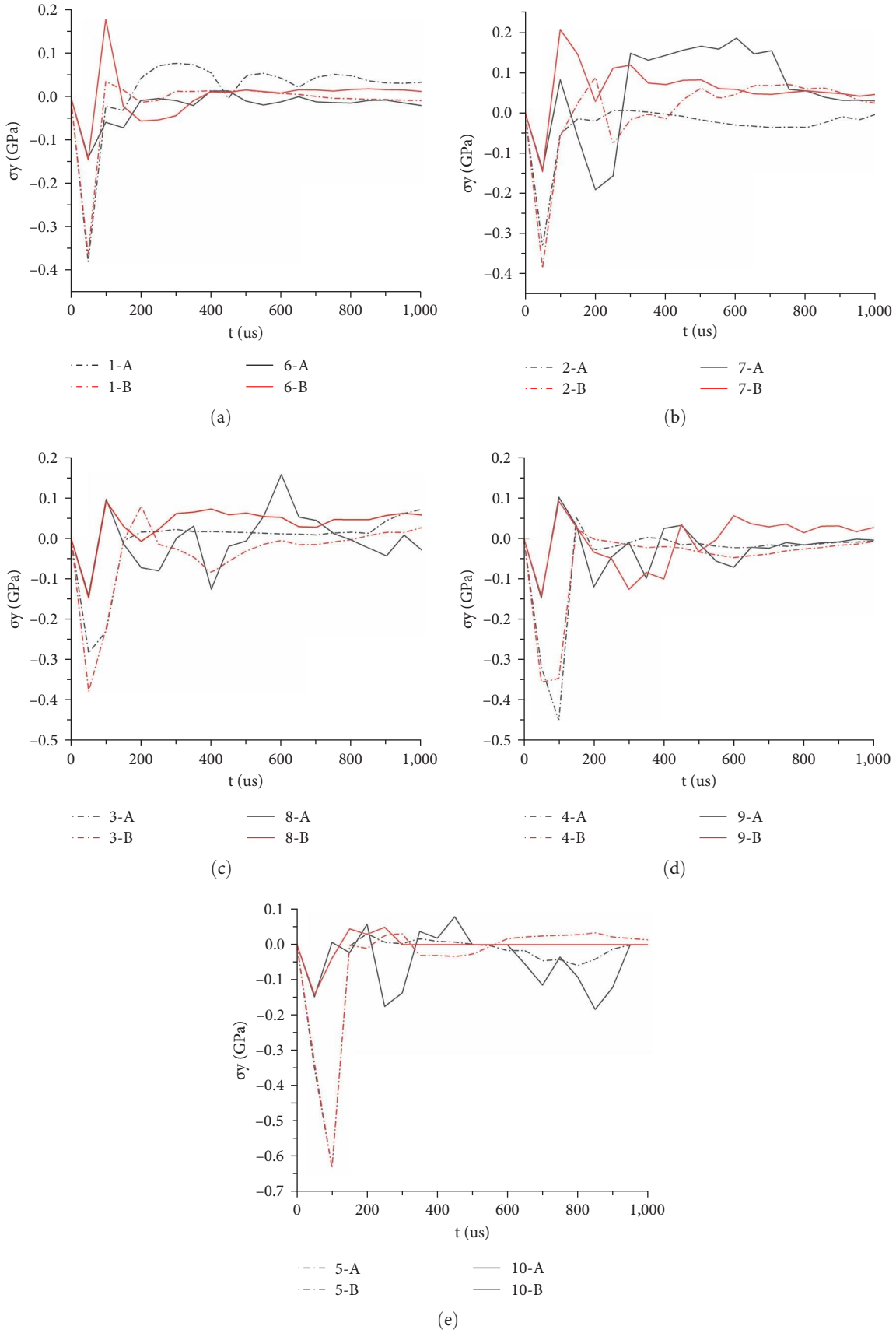

Figure 11: *Y*-direction stress variation curve: (a) charge diameter 32 mm, (b) charge diameter 36 mm, (c) charging diameter 40 mm, (d) charging diameter 44 mm, and (e) charge diameter 48 mm.

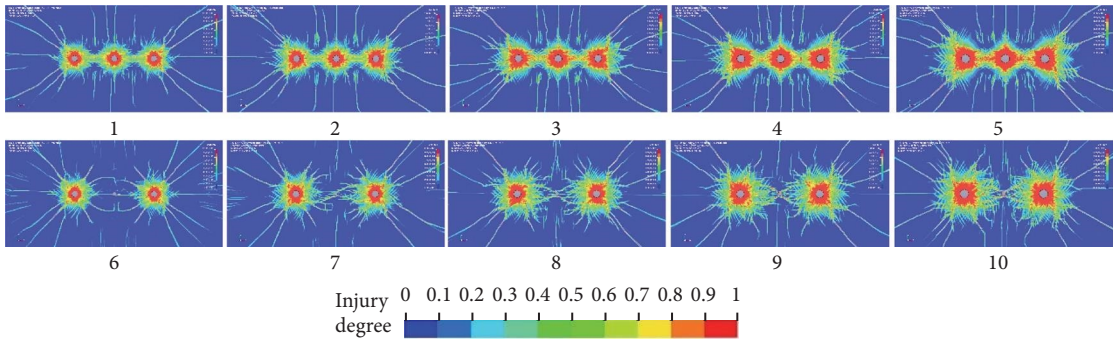

Figure 12: Effect of damage to the gun hole after blasting with different schemes.

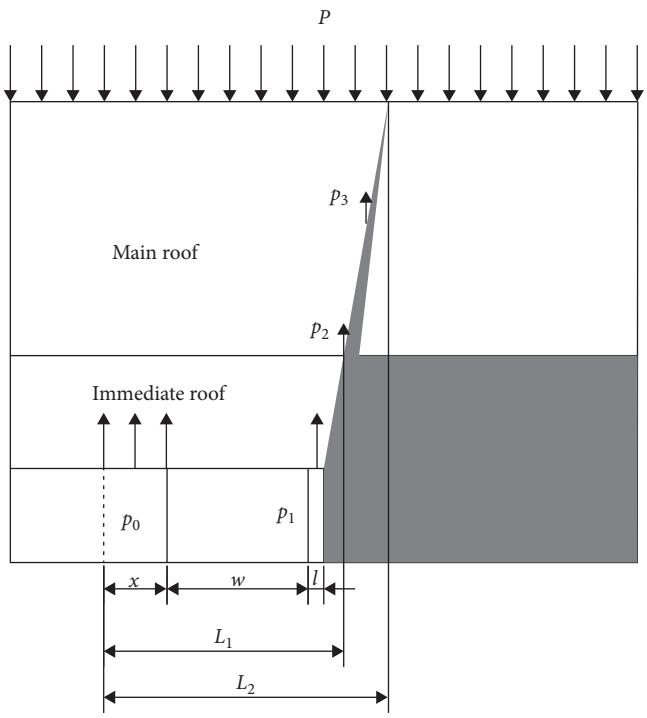

Figure 13: Mechanical model of the roadway.

$$p_0 x + p_1 l + p_2 l_1 + p_3 l_2 = \gamma_1 m_1 L_1 + \gamma_2 m_2 L_2, \tag{12}$$

where l_1 is gangue on the direct top of the action length, l_2 is gangue on the main roof of the action length, γ_1 is the main roof capacity, m_1 is the main roof thickness, L_1 is the main roof hanging length, γ_2 is the immediate roof capacity, m_2 is the immediate roof thickness, and L_2 is the immediate roof hanging length.

Since p_0 is the residual compressive strength of the roadway gang, let the stress concentration factor be K, then

$$p_1 = \frac{K}{l}[\gamma_1 m_1 L_1 + \gamma_2 m_2 L_2 - P_x x_0 - p_2 l_1 - p_3 l_2]. \tag{13}$$

According to the theory of elastic foundation, there are

$$\begin{cases} p_2 = \dfrac{1}{2}\gamma_2 m_2 \\ p_3 = \dfrac{1}{2}\gamma_1 m_1 \end{cases}. \tag{14}$$

By obtaining the relevant parameters through onsite investigation, $K = 2$, $l = 0.25$ m, $\gamma_1 = 26.8$ kN/m^3, $m_1 = 8.1$ m, $L_1 = 36.46$ m, $\gamma_2 = 26$ kN/m^3, $m_2 = 3.6$ m, $L_2 = 6.65$ m, $P_x = \sigma_c = 0.72$ MPa, $\lambda = 1.5$, $m = 3$ m, $\varphi = 38°$, $k = 2$, $\gamma = 16$ kN/m^3, and $H = 650$ m. Substituting into Equations (11) and (13) yields $p_1 = 30.84$ MPa. Therefore, the bearing capacity, p_s of the roadside support should be greater than 30.84 MPa, that is $p_s > p_1$.

4. Countermeasures for Roadway Support

4.1. Gob-Side Entry Retaining Support Program. "Anchor rod (cable) + anchor network" is used in the roadway. There are six anchor rods in each row on the roof of the roadway and three anchor rods on each side of the roadway with a distance of 900 mm. Four cables are laid on the roof of the roadway with a distance of 1,800 mm between the two rows of anchor rods. Wire mesh is laid continuously on the roof of the roadway and on the left and right sides of the roadway. Within 50 m ahead of the working face, single hydraulic pillar is set up in the roadway as overrun support, the pillar is set up as shown in Figure 14, the row distance is 800 mm. steel pipe concrete pillar is set up at the back side of the working face, the row distance is 800 mm, and the bamboo curtain is pulled between the pillars and the slurry is sprayed to seal the mining area. At the back of the working face, a steel pipe concrete pillar is erected at the middle axis of the 20 m roadway, the row distance is 800 mm, and the single hydraulic pillar is withdrawn.

4.2. Application Effect. According to the above numerical simulation, the diameter of the emulsion explosive used in the test section of the roadway roof cutting is Φ40 mm × 330 mm/roll, using Φ40-mm PVC pipe to charge the explosive, the mass of each section of explosive is 300 g, the charge of

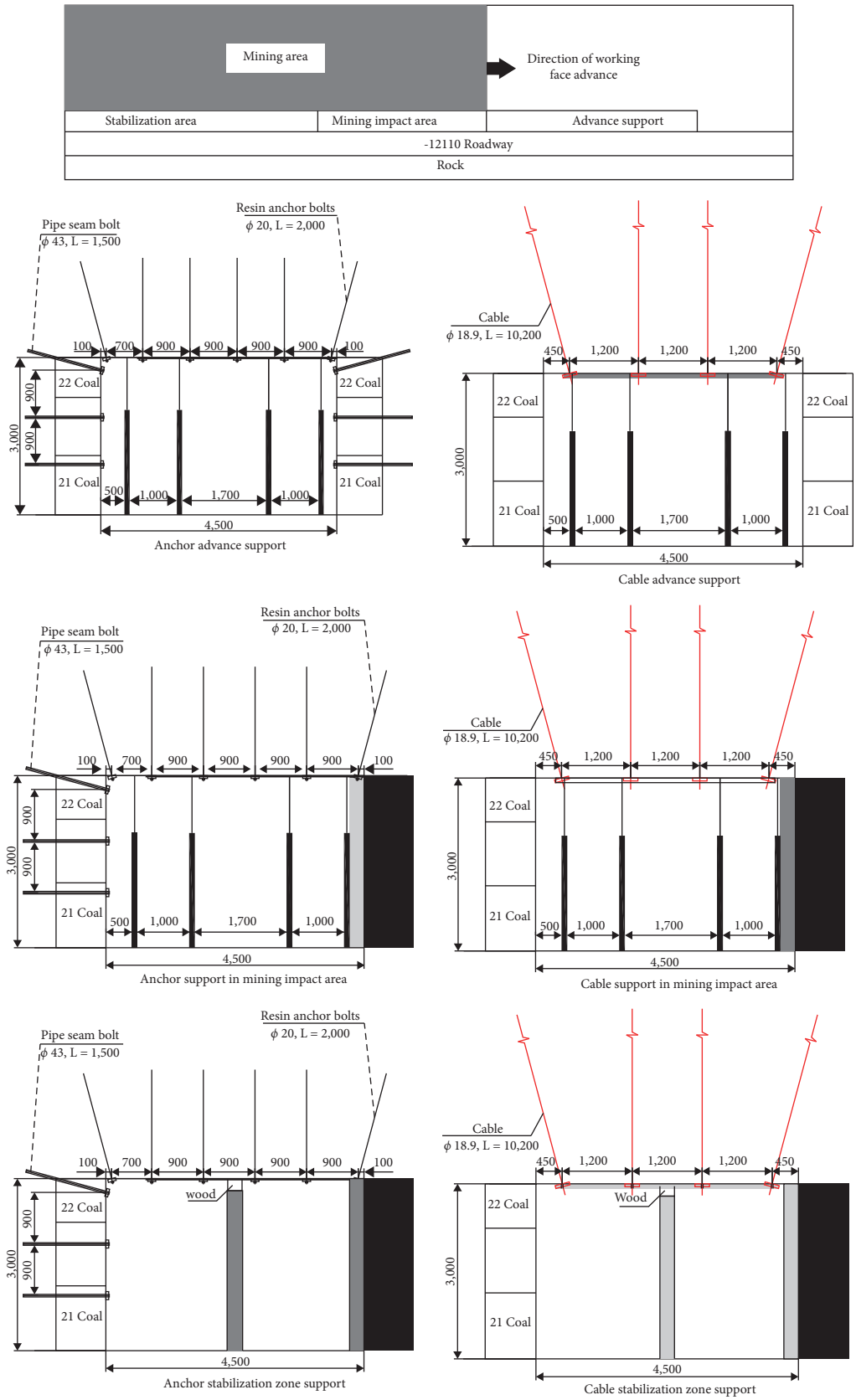

FIGURE 14: Delineate area support.

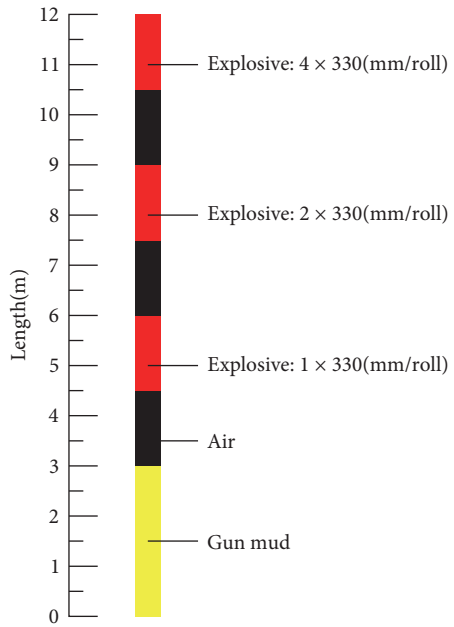

Figure 15: Gun hole charging scheme.

Figure 16: Drill hole peeper observation results.

Figure 17: Preparation of steel pipe concrete columns.

each blasting hole is 2.1 kg, and the charging method is shown in Figure 15. Using interval loading, each blast is 1 m in length along the roadway, and two holes are blasted simultaneously. Since the cracks formed in the roof could not be observed directly after blasting, and it was not easy to observe the presence of fuses and gun clay in the charge holes, the CXK12 borehole peeper was used on site to observe the empty holes, as shown in Figure 16.

Based on the results of the above study, a field test was conducted at the Xiaohezui coal mine -12110 working face in Sichuan, as shown in Figures 17 and 18. The main component of the roadside support is the steel pipe concrete column. Steel

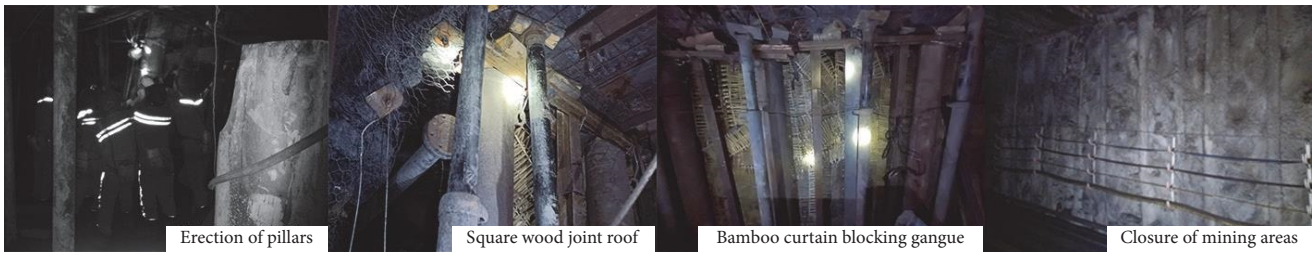

Figure 18: Roadway side support.

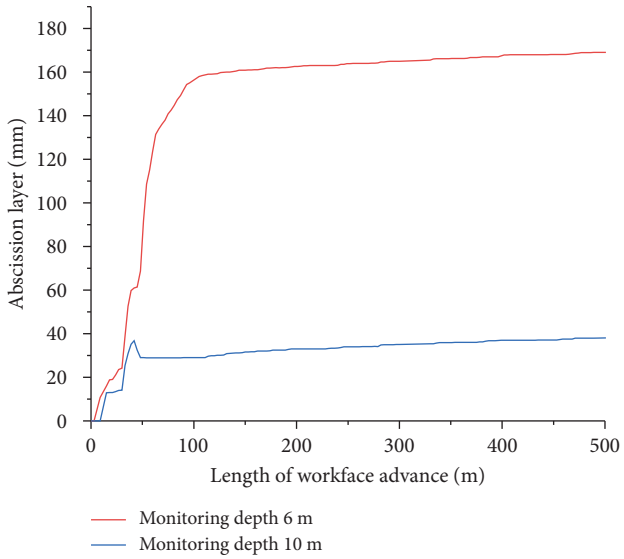

Figure 19: Trend of the roof-plate delamination of the roadway.

tube length is 2,750 mm and diameter is 10 inches. It is grouted and sealed on the ground (The standard value of compressive strength of concrete is 50 MPa) and transported to the working face for erection after 28 days of maintenance, and a wooden block with a thickness of 250 mm is wedged between the top plate and the pipe column for the erection. After the pillars are erected, bamboo gabions are hung between the pillars to block the rock refuse and shotcrete slurry to ensure that the roadway is sealed.

Rock movement sensors are installed at the roof of the test section 20 m ahead of the workface. The roof of the roadway is observed continuously to verify the effectiveness of the roof cutting. The measurement points are arranged at 1 m on the roof of the roadway near the coal wall side of the workface, and the depths are 6 and 10 m, respectively, and the accumulation of the abscission layer change starts from the workface advancing to the monitoring point. The observation results of the roof separation of the roadway are shown in Figure 19. After adjusting the blasting parameters, the roof separation was controlled within 180 mm, and deformation of the roadway envelope is controlled.

5. Conclusion

(1) Numerical simulation results show that effective cracks can be formed between blast holes during adjacent blasting. But the lower the charge uncoupling factor, the larger the perimeter of the hole crushing zone, which is not conducive to the maintenance of the roof of large sections of roadway. When the charge diameter is 40 mm and above, the effective crack can be formed between the interval blasting holes, and as the charge uncoupling coefficient decreases, the more obvious the guiding effect of the uncharged holes, the larger the perimeter of the blasting hole crushing zone.

(2) The mechanics model of large section soft-rock roadway was established, the support resistance equation of the support next to the roadway and the gangue in the mining area to the roof rock was derived, and the minimum support resistance of the support was obtained as 30.84 MPa.

(3) The field test results show that when the diameter of emulsified explosive is Φ40 mm × 330 mm/roll, using Φ40-mm PVC pipe loading, the mass of the explosive is 300 g per section, and the loading quantity of each blasting hole is 2.1 kg, continuous cracks can be formed between holes.

(4) According to the influence range of dynamic pressure and cycle pressure law, the support scheme of different areas is proposed, and the deformation of surrounding rock is controlled after field application.

Conflicts of Interest

The authors declare that they have no conflicts of interest.

Acknowledgments

The authors received funding from the National Natural Science Foundation of China (Grants: 52174110, 52274119) and the Hunan Provincial Natural Science Foundation of China (Grant: 2021JJ30273).

References

[1] S. K. Zhao, Q. X. Qi, Y. P. Li, Z. G. Deng, Y. Z. Li, and Z. G. Su, "Theory and practice of rockburst stress control technology in deep coal mine," *Journal of China Coal Society*, vol. 45, no. s2, pp. 626–636, 2020.

[2] G. Feng, X. Wang, M. Wang, and Y. Kang, "Experimental investigation of thermal cycling effect on fracture characteristics of granite in a geothermal-energy reservoir," *Engineering Fracture Mechanics*, vol. 235, Article ID 107180, 2020.

[3] Q. Wu, X. Li, L. Weng, Q. Li, Y. Zhu, and R. Luo, "Experimental investigation of the dynamic response of prestressed rockbolt by using an SHPB-based rockbolt test system," *Tunnelling and Underground Space Technology*, vol. 93, Article ID 103088, 2019.

[4] X. H. Xu, F. L. He, K. Lv, D. Q. Wang, L. Li, and W. L. Zhai, "Research on reasonable cutting roof parameters of gob side entry retaining by roof cutting in thick and hard roof," *Journal of China Coal Society*, vol. 48, no. 8, pp. 3048–3059, 2023.

[5] J. G. Guo, Y. H. Li, S. H. Shi et al., "Self-forming roadway of roof cutting and surrounding rock control technology under thick and hard basic roof," *Journal of China Coal Society*, vol. 46, no. 9, pp. 2853–2864, 2021.

[6] Y. B. Gao, J. Yang, Q. Wang, Y. J. Wang, and M. C. He, "Mechanism of roof presplitting in a nonpillar mining method with entry automatically retained and its influence on the strata behaviors," *Journal of China Coal Society*, vol. 44, no. 11, pp. 3349–3359, 2019.

[7] P. Li, Y. J. Zhu, P. Wang et al., "Study on reasonable width and yield scale of roadway side support with strong roof and thick seam with large dip angle," *Journal of Central South University (Science and Technology)*, vol. 53, no. 11, pp. 4494–4503, 2022.

[8] G. Feng, X. Wang, Y. Kang, and Z. Zhang, "Effect of thermal cycling-dependent cracks on physical and mechanical properties of granite for enhanced geothermal system," *International Journal of Rock Mechanics and Mining Sciences*, vol. 134, Article ID 104476, 2020.

[9] Q. Wu, L. Chen, B. Shen, B. Dlamini, S. Li, and Y. Zhu, "Experimental investigation on rockbolt performance under the tension load," *Rock Mechanics and Rock Engineering*, vol. 52, no. 11, pp. 4605–4618, 2019.

[10] M. C. He, P. F. Guo, X. H. Zhang, and J. Wang, "Directional pre-splitting of roadway roof based on the theory of bilateral cumulative tensile explosion," *Explotion and Shock Wave*, vol. 93, no. 4, pp. 795–803, 2018.

[11] S. Y. Chen, F. Zhao, H. J. Wang, G. X. Yuan, Z. B. Guo, and J. Yang, "Determination of key parameters of gob-side entry retaining by cutting roof and its application to a deep mine," *Rock and Soil Mechanics*, vol. 40, no. 1, pp. 332–342, 2019.

[12] J. Wei, "Numerical simulation on contribution of guide-hole to crack coalescence of two boreholes," *Engineering Mechanics*, vol. 30, no. 5, pp. 335–339, 2013.

[13] Y. Chen, S. P. Hao, Y. T. Chen, Z. Z. Zhang, L. F. Wu, and H. L. Liu, "Study on the application of short-hole blasting with guide hole to roof cutting pressure relief of gob-side entry retaining," *Journal of Mining and Safety Engineering*, vol. 32, no. 2, pp. 253–259, 2015.

[14] M. Tu, G. Zhao, X. Zhang, Q. Bu, and J. Dang, "Fracture evolution between blasting roof cutting holes in a mining stress environment," *Minerals*, vol. 12, no. 4, Article ID 418, 2022.

[15] M. C. He, S. Y. Chen, Z. B. Guo, J. Yang, and Y. B. Gao, "Control of surrounding rock structure for gob-side entry retaining by cutting roof to release pressure and its engineering application," *Journal of China University of Mining & Technology*, vol. 46, no. 5, pp. 959–969, 2017.

[16] Y. J. Wang, M. C. He, K. X. Zhang et al., "Strata behavior characteristics and control countermeasures for the gateroad surroundings in innovative non-pillar mining method with gateroad formed automatically," *Journal of Mining and Safety Engineering*, vol. 35, no. 4, pp. 677–685, 2018.

[17] H.-P. Rossmanith, *Rock Fracture Mechanics*, Springer Science and Business Media, 1983.

[18] M. C. He and X. M. Sun, *Design and Construction Guidelines for Soft Rock Tunnel Engineering Support in Chinese Coal Mines*, Science Press, 2004.

[19] K. Gao, Z. G. Liu, J. Liu et al., "Application of deep borehole blasting to gob-side entry retaining forced roof caving in hard and compound roof deep well," *Chinese Journal of Rock Mechanics and Engineering*, vol. 32, no. 8, pp. 1588–1594, 2013.

[20] M. G. Qian, P. W. Shi, and J. L. Xu, *Ground Pressure and Strata Control*, China University of Mining and Technology press, 2010.

[21] T. Borrvall and W. Riedel, "The RHT concrete model in LS-DYNA," in *8th European LS-DYNA Users Conference*, pp. 1–14, Strasbourg, 2011.